



# Electroresponsive Structurally Colored Materials: A Combination of Structural and Electrochromic Effects

Tomoya Kuno, Yoshimasa Matsumura, Koji Nakabayashi, and Mahito Atobe\*

**Abstract:** Electroresponsive structurally colored materials composed of ordered arrays of polyaniline@poly(methyl methacrylate) (PANI@PMMA) core-shell nanoparticles have been successfully prepared. The core-shell nanoparticles were synthesized by deposition of PANI shells on the surfaces of the PMMA cores by the oxidative polymerization of anilinium chloride. Ordered arrays were then fabricated by using the fluidic cell method. Because the ordered arrays and the PANI shells generate structural and electrochromic colors, respectively, these core-shell colloidal crystals exhibited colors resulting from the combined effects of these materials. The crystal colors depended greatly on the size of PANI@PMMA particles and could also be varied by the application of a voltage. The electrochromic colors of these arrays were found to be quite different from those exhibited by pure PANI films prepared by electrochemical oxidation.

Hybrid nanomaterials are composites that consist of two or more compounds interspersed at the nanometric level.<sup>[1,2]</sup> These materials differ from traditional composites in which the constituents are combined on a macroscopic level. Mixing on the nanometer scale generates materials that have greater homogeneity and that exhibit characteristics that lie between those of the original phases or, in some cases, entirely new properties. A core-shell nanoparticle is composed of a core made of one material that has been coated with another substance, and such particles represent hybrid nanomaterials with a greater variety of promising applications compared with single-phase nanoparticles.<sup>[3–5]</sup>

A photonic crystal is a periodic optical nanostructure; such crystals are commonly applied as structurally colored materials. Because the structural color imparted by a photonic crystal is generated based on a different principle from the color obtained from a pigment, these crystals have been widely studied as new sources of color.<sup>[6,7]</sup> In addition, the structural color can be dynamically manipulated by external sources such as electrical,<sup>[8]</sup> chemical,<sup>[9]</sup> thermal,<sup>[10]</sup> or mechanical stimuli,<sup>[11]</sup> and therefore a large number of

stimuli-responsive photonic crystals have been developed in recent years.<sup>[12,13]</sup> However, most of their color manipulation is based on the modification of the periodicity of the photonic crystals with external stimuli.

Conducting polymers such as polyaniline (PANI) are known to exhibit unique electrochromic properties<sup>[14–17]</sup> and have been identified as potential components of electrochromic devices.<sup>[18–21]</sup> However, the colors that can be obtained from these materials are solely decided by the type of polymer employed, and hence their color range is relatively limited.

Based on this background information, we predicted that combinations of structurally colored photonic crystals and electrochromically colored conducting polymers would produce new chromic colors. Therefore we prepared ordered arrays of PANI@PMMA core-shell nanoparticles (PMMA = poly(methyl methacrylate) with the aim of developing novel electroresponsive structurally colored materials. The color manipulation upon electrical stimulus was not based on the modification of the crystal periodicity but on the electrochromism of the PANI layer of the composites.

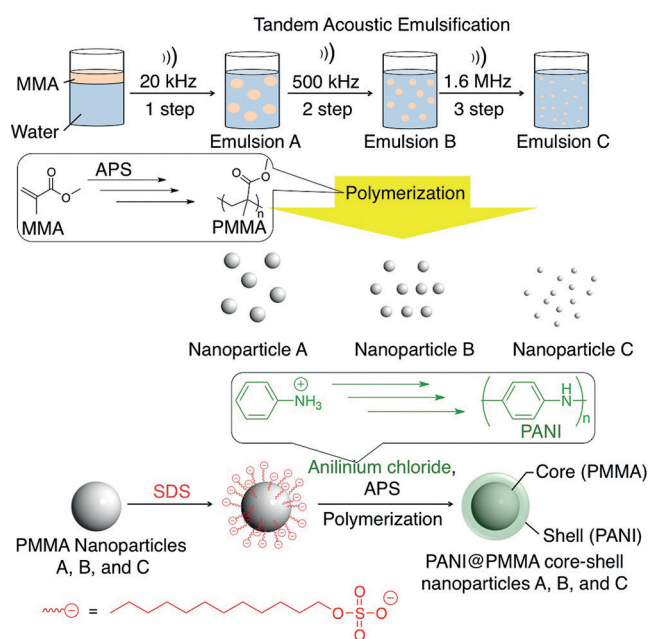
To accomplish this goal, we initially prepared size-controlled PMMA nanoparticles for use as the core units within core-shell nanoparticles, and employed soap-free emulsion polymerization in conjunction with tandem acoustic emulsification.<sup>[22,23]</sup> This synthetic method involved sequential ultrasonic irradiation (20 kHz → 500 kHz → 1.6 MHz) to obtain the acoustic emulsification of the water-insoluble MMA monomer in an aqueous medium (Figure 1a). The resulting emulsions were subsequently heated to initiate radical polymerization in the presence of ammonium persulfate (APS; emulsions A, B, and C in Figure 1a). By using this method we were able to obtain three different sizes of PMMA nanoparticles (A, B and C, with average sizes of 248, 220, and 201 nm, respectively; Figure 1a). Polyaniline was subsequently deposited on the surfaces of the PMMA cores by the oxidative polymerization of anilinium chloride with APS in core particle suspensions to obtain PANI@PMMA core-shell nanoparticles (Figure 1b). During this process, the PMMA particle surfaces were negatively charged through the addition of a small amount of sodium dodecyl sulfate to allow the effective deposition of PANI, which is positively charged.<sup>[24,25]</sup>

Figure 2 shows SEM and TEM images of the obtained PMMA and PANI@PMMA core-shell nanoparticles. Although both types of particles appear essentially the same size in the SEM images (Figure 2a,b), 5–15 nm thick PANI outer layers can be observed in the TEM images of the PANI@PMMA core-shell nanoparticles (Figure 2d). Furthermore, characteristic absorption bands for both PMMA

[\*] T. Kuno, Dr. Y. Matsumura, Prof. Dr. M. Atobe  
Department of Environment and System Sciences  
Yokohama National University  
79-7 Tokiwadai, Hodogaya-ku, Yokohama 240-8501 (Japan)  
E-mail: atobe@ynu.ac.jp

Dr. K. Nakabayashi  
Institute for Materials Chemistry and Engineering  
Kyushu University  
6-1 Kasuga-koen, Kasuga-city, Fukuoka 816-8580 (Japan)

Supporting information for this article is available on the WWW under <http://dx.doi.org/10.1002/anie.201511191>.



**Figure 1.** Preparation of a) PMMA nanoparticles and b) PANI@PMMA core-shell nanoparticles.

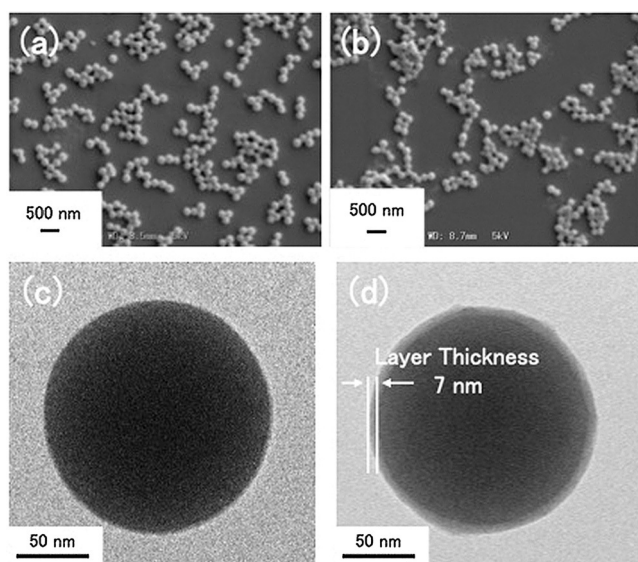


**Figure 2.** SEM and TEM images of PMMA nanoparticles C and PANI@PMMA core-shell nanoparticles C: a) SEM image of PMMA nanoparticles, b) SEM image of PANI@PMMA core-shell nanoparticles, c) TEM image of PMMA nanoparticles, and d) TEM image of PANI@PMMA core-shell nanoparticles.

and PANI were observed in the IR spectrum of the PANI@PMMA core-shell nanoparticles (Figure 3). From these results, it can be concluded that the obtained nanoparticles have a core-shell morphology composed of PMMA and PANI.

We next fabricated colloidal crystal films composed of variously sized PANI@PMMA core-shell nanoparticles by using the fluidic cell method.<sup>[26]</sup> Upon injection of a PANI@PMMA core-shell nanoparticle solution into the cell

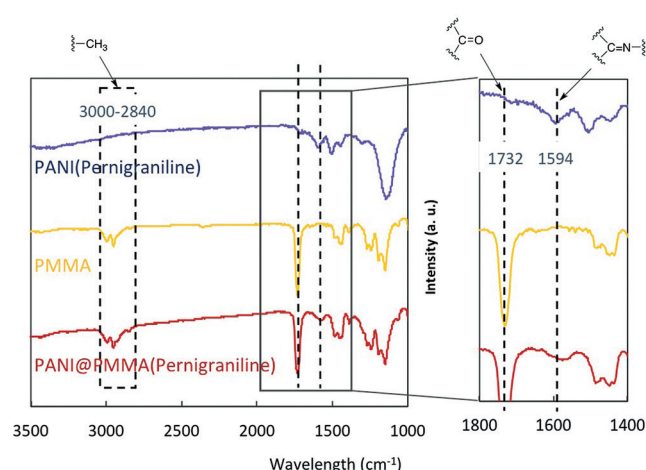


**Figure 3.** IR spectra of a) PANI prepared by the oxidative polymerization of anilinium chloride with APS, b) PMMA nanoparticles, and c) PANI@PMMA core-shell nanoparticles.

reservoir, the core-shell spheres dispersed throughout the fluidic cell as the result of capillary action. Colloidal crystal films exhibiting structural color gradually grew from the vicinity of the opposite opening of the cell.

Photographic images of PANI@PMMA colloidal crystal films formed within a fluidic cell are shown in Figure 4. It is evident that the various film samples exhibited different optical properties. Film A, composed of the A-type PANI@PMMA core-shell particles, had a greenish-yellow coloration, while film B, composed of the B particles, exhibited a light-green coloration, and film C (C particles) was light-blue. The SEM images of these films clearly show densely packed structures that comprise periodic arrays of the PANI@PMMA core-shell particles. According to Bragg's equation, when the film is composed of the smaller-size particles, the interparticle distance should be narrower. Therefore the reflection color was blue-shifted on changing from films A to C. In addition, the reflection colors of all crystal samples showed an angle dependency (see Figure S4 in

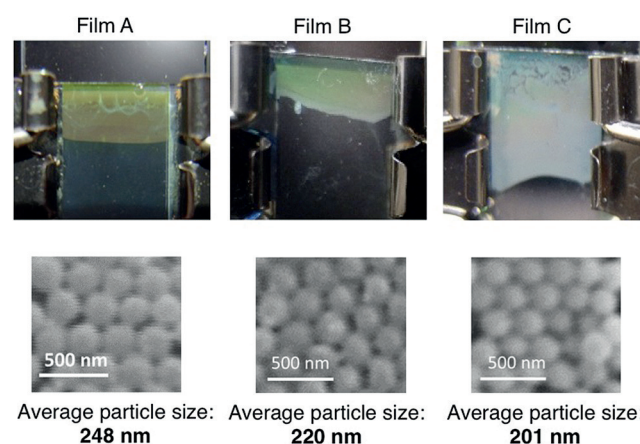


**Figure 4.** Photographic and SEM images of colloidal crystal films composed of PANI@PMMA core-shell nanoparticles. The PANI layers are in the emeraldine state.

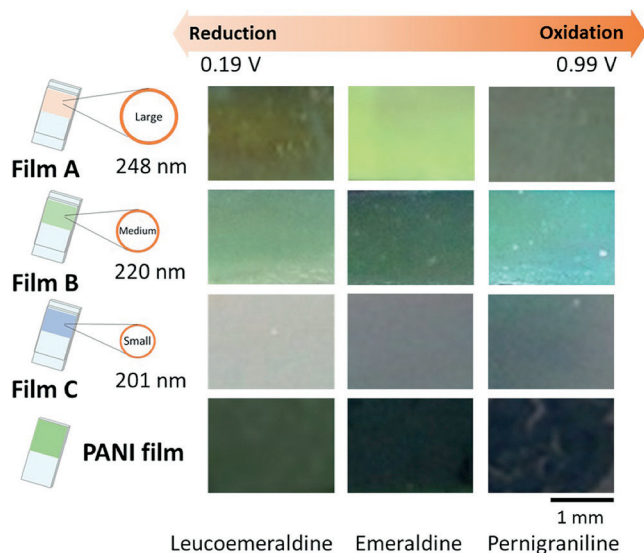


**Figure 5.** Electrochromic properties of the A, B and C colloidal crystal films and the PANI film.

the Supporting Information). The vivid coloration of these films actually depends on their highly ordered structures.

Subsequently, voltages were applied to the three colloidal crystal films in order to evaluate their electrochromic properties. As expected, the PANI@PMMA colloidal crystals exhibited electrochromic properties as a result of the conductive PANI layer in each film (Figure 5). As an example, the color of film A changed from yellowish-green to dull orange at 0.19 V because of the reduction of the PANI layer, which induced the formation of the leucoemeraldine state. In contrast, film A transitioned to grayish-blue at 0.99 V because of the associated oxidation of the PANI layer. Films B and C also underwent unique color changes based on the redox state of the PANI layer. These electrochromic color changes were quite different from those typically demonstrated by pure PANI. By applying a voltage, the particles might move and arrange in an ordered structure; this phenomenon also affects color changes. To check this possibility, we observed the surface of the colloidal crystal films after the applying voltages of 0.19 and 0.99 V. As results, the sizes and arrangements of the particles were mostly maintained as colloidal crystals even after applying the voltages (see Figure S5 in the Supporting Information). It can be therefore confirmed that the color manipulation with an electrical stimulus depends mainly on the electrochromism of the PANI layers.

To evaluate the color manipulation with an electrical stimulus in more detail, we subsequently acquired reflection spectra from the colloidal crystal films as well as a PANI film prepared by electrochemical polymerization (Figure 6). It is surprising that the reflection spectra of the colloidal crystal films were completely different from those observed for bulk PANI. In addition, the spectra of the three colloidal crystal films also differ from each other. However, they seem to exhibit similar trends in the peak shift by electrical stimulus, that is, transitioning the PANI layer to the leucoemeraldine state by electroreduction induced a bathochromic shift in the

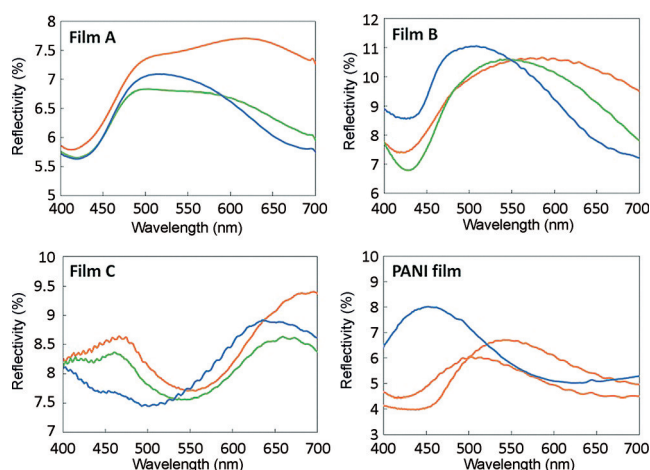


**Figure 6.** Reflection spectra of films A, B, C and the polyaniline film (blue: peroxidized state (pernigraniline), green: oxidized state (emeraldine salt) and red: reduced state (leucoemeraldine)).

reflection spectrum because of the associated color changes of the film. In contrast, the spectra were hypsochromically shifted when the PANI layer was oxidized to its pernigraniline state. The particle-size-dependence might also be evaluated from the spectra taken from the same redox state. Figure 7 shows the reflection spectra of films A, B, and C in the pernigraniline state. By comparing these spectra, it was confirmed that the spectrum blue-shifted on going from films A to C. This trend is consistent with that observed in the photographic images.

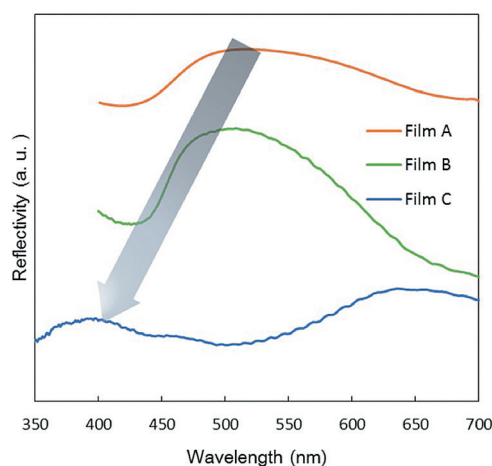


**Figure 7.** Reflection spectra of films A, B, and C in the pernigraniline state.

At present, a reliable mechanism for such unique color changes in the colloidal crystals can not be proposed. However, it can be concluded that both the ordered arrays and the PANI layers contribute significantly to such unique color effects. The preparation of electroresponsive structurally colored materials composed of ordered arrays of other core-shell nanoparticles and their systematic characterization are in progress in order to propose a reliable mechanism.



In conclusion, we were able to prepare a number of electroresponsive structurally colored materials. These materials were made of ordered arrays of PANI@PMMA core-shell nanoparticles and showed both structural and electrochromic coloration. The present method is clearly a powerful tool for the preparation of new colored materials.

### Acknowledgements

The authors are grateful to Dr. Masashi Kondo of the Instrumental Analysis Center at Yokohama National University for his kind assistance with the TEM analyses. This work was partially supported by a Grant-in-Aid for Scientific Research (15H03843).

**Keywords:** colloidal crystals · conducting polymers · electrochromism · nanoparticles · structural colors

**How to cite:** *Angew. Chem. Int. Ed.* **2016**, *55*, 2503–2506  
*Angew. Chem.* **2016**, *128*, 2549–2552

- 
- [1] C. He, D. Liu, W. Lin, *Chem. Rev.* **2015**, *115*, 11079.  
[2] S. Sacanna, W. T. M. Irvin, P. M. Chaikin, D. J. Pine, *Nature* **2010**, *464*, 575.  
[3] K. E. Sapsford, W. R. Alger, L. Berti, K. B. Gemmill, B. J. Casey, E. Oh, M. H. Stewart, I. L. Medintz, *Chem. Rev.* **2013**, *113*, 1904.  
[4] Y. Gotoh, H. Sukuki, N. Kumano, T. Seki, K. Katagiri, Y. Takeoka, *New J. Chem.* **2012**, *36*, 2171.  
[5] S. Yang, C. Song, T. Qiu, L. Guo, X. Li, *Langmuir* **2013**, *29*, 92.  
[6] J. E. Stumpel, D. J. Broer, A. P. H. J. Schenning, *Chem. Commun.* **2014**, *50*, 15839.  
[7] J. Ge, Y. Yin, *Angew. Chem. Int. Ed.* **2011**, *50*, 1492; *Angew. Chem.* **2011**, *123*, 1530.  
[8] D. P. Puzzo, A. C. Arsenault, I. Manners, G. A. Ozin, *Angew. Chem. Int. Ed.* **2009**, *48*, 943; *Angew. Chem.* **2009**, *121*, 961.  
[9] J. H. Holtz, S. A. Asher, *Nature* **1997**, *389*, 829.  
[10] Y. Takeoka, M. Watanabe, *Langmuir* **2003**, *19*, 9104.  
[11] H. Fudouzi, T. Sawada, *Langmuir* **2006**, *22*, 1365.  
[12] L. Nucara, F. Greco, V. Mattoli, *J. Mater. Chem. C* **2015**, *3*, 8449.  
[13] J. Zhang, C. Chu, A. Sun, S. Ma, X. Qiao, C. Wang, J. Guo, Z. Li, G. Xu, *J. Alloys Compd.* **2016**, *654*, 251.  
[14] P. M. Beaujuge, J. R. Reynolds, *Chem. Rev.* **2010**, *110*, 268.  
[15] A. Watanabe, K. Mori, Y. Iwasaki, Y. Nakamura, *Macromolecules* **1987**, *20*, 1793.  
[16] S. K. Dhawan, M. K. Ram, B. D. Malhotra, S. Chandra, *Synth. Met.* **1995**, *75*, 119.  
[17] A. Cihaner, F. Algi, *Electrochim. Acta* **2008**, *54*, 665.  
[18] A. A. Argun, P. H. Aubert, B. C. Thompson, I. Schwendeman, C. L. Gaupp, J. Hwang, N. J. Pinto, D. B. Tanner, A. G. MacDiarmid, J. R. Reynolds, *Chem. Mater.* **2004**, *16*, 4401.  
[19] M. T. Otley, F. A. Alamer, Y. Zhu, A. Singhaviranon, X. Zhang, M. Li, A. Kumar, G. A. Sotzing, *ACS Appl. Mater. Interfaces* **2014**, *6*, 1734.  
[20] P. Chandrasekhar, B. J. Zay, G. C. Birur, S. Rawal, E. A. Pierson, L. Kauder, T. Swanson, *Adv. Funct. Mater.* **2002**, *12*, 95.  
[21] D. M. DeLongchamp, P. T. Hammond, *Chem. Mater.* **2004**, *16*, 4799.  
[22] K. Nakabayashi, M. Kojima, S. Inagi, Y. Hirai, M. Atobe, *ACS Macro Lett.* **2013**, *2*, 482.  
[23] Y. Hirai, M. Koshino, Y. Matsumura, M. Atobe, *Chem. Lett.* **2015**, *44*, 1584.  
[24] M. S. Cho, Y. H. Cho, H. Y. Choi, M. S. John, *Langmuir* **2003**, *19*, 5785.  
[25] Y. D. Liu, F. F. Fang, H. J. Choi, *Langmuir* **2010**, *26*, 12849.  
[26] M. Ishii, H. Nakamura, H. Nakano, A. Tsukigase, M. Harada, *Langmuir* **2005**, *21*, 5367.
- 

Received: December 3, 2015

Published online: January 12, 2016